

# Sustainable PHBV/CuS Composite Obtained from Waste Valorization for Wastewater Purification by Visible Light-Activated Photocatalytic Activity

Gabriele Sarapajevaite,\* Kestutis Baltakys, Micaela Degli Esposti, Davide Morselli,\* and Paola Fabbri

The persistency of antimicrobial compounds in the water cycle accelerates the issue of antimicrobial resistance. Therefore, effective wastewater remediation approaches, which can be implemented on a large scale, are urgently required. This study aims at preparing a sustainable organic/inorganic composite material that can photo-catalyze the degradation of organic pollutants in wastewater by using visible light. Specifically, films and porous composites are composed of poly(3-hydroxybutyrate-co-3-hydroxyvalerate) (PHBV) as supporting material, and copper sulfide (CuS) as active photocatalyst. It is noteworthy that the proposed composite can be fully produced from waste valorization, since PHBV is a polymer, which can be obtained by fermentation of vegetable wastes, and CuS is synthesized from industrial sulfur wastes. The produced composites show remarkable capabilities in the photodegradation of tetracycline and methylene blue, selected as model organic pollutants. Moreover, the PHBV/CuS composites can be reused multiple times with minimal loss in photocatalytic efficiency. The suggested approach is not only sustainable and cost-effective, but also solves issues occurring in the application of the photodegradation techniques currently reported, such as the consumption of fossil-based chemicals and photocatalyst removal from the purified water using with expensive procedures.

## 1. Introduction

More than 2 billion of the human population use water contaminated with excrement, confirming that clean drinking water supply to all human beings is still an unresolved issue throughout the globe.<sup>[1]</sup> For this reason, the United Nations has proposed the sixth sustainable development goal (SDG) to highlight that the clean water supply for everyone is an urgent call for action by all countries—developed and developing—in a global partnership. In particular, one of the main targets of the mentioned SDG is to halve the amount of hazardous compounds in untreated wastewater until 2030.<sup>[2]</sup> One of the main pollutants found in underground and surface waters is antimicrobial compounds, such as antibiotics, which are introduced into wastewater due to human consumption or as antimicrobial manufacturing waste.<sup>[1]</sup> Moreover, antimicrobial compounds are broadly applied in agriculture,

livestock farming, and aquaculture, consequently causing the human body as the center of the antibiotic provision cycle.<sup>[3]</sup> It has been reported that even 80% of administered antimicrobial substances are emitted as active metabolites in human feces that are also collected by wastewater.<sup>[1,3]</sup> The applied conventional wastewater remediation processes are usually ineffective since the detected amount of antibiotics in purified wastewater has been increasing in recent years.<sup>[1,3]</sup> As a consequence of the constant exposure to antimicrobial compounds in the environment, the unforeseen acceleration of human antimicrobial resistance has become a major issue of healthcare systems worldwide.<sup>[4,5]</sup>

The development of novel solutions to degrade antibiotics in wastewater is crucial, therefore several emerging technologies have been recently proposed. Among them, adsorption processes using carbon-based adsorbents (graphene-based membranes, activated granular powders) have been widely investigated.<sup>[6,7]</sup> A growing number of research groups are focusing on physicochemical processes for antibiotic degradation, such as electrochemical oxidation, ozonation, and the Fenton process, since only harmless compounds emerge as pollutant degradation

G. Sarapajevaite, K. Baltakys  
Department of Silicate Technology  
Kaunas University of Technology  
Radvilenu Road 19, Kaunas LT-50254, Lithuania  
E-mail: gabriele.sarapajevaite@ktu.lt

G. Sarapajevaite, M. Degli Esposti, D. Morselli, P. Fabbri  
Department of Civil, Chemical, Environmental, and Materials Engineering (DICAM)  
Università di Bologna  
Via Terracini 28, Bologna 40131, Italy  
E-mail: davide.morselli6@unibo.it

M. Degli Esposti, D. Morselli, P. Fabbri  
National Interuniversity Consortium of Materials Science and Technology (INSTM)  
Via Giusti 9, Firenze 50121, Italy

 The ORCID identification number(s) for the author(s) of this article can be found under <https://doi.org/10.1002/adsu.202300112>

© 2023 The Authors. Advanced Sustainable Systems published by Wiley-VCH GmbH. This is an open access article under the terms of the Creative Commons Attribution License, which permits use, distribution and reproduction in any medium, provided the original work is properly cited.

DOI: 10.1002/adsu.202300112

products in the presence of generated strong oxidizing radicals.<sup>[8]</sup> Due to the relatively low processing cost and the developed high degradation efficiency (DE), photocatalysts as metal oxides (e.g., TiO<sub>2</sub> and ZnO), metal chalcogenides (e.g., NiS, MoS<sub>2</sub>, and CuS), or metallic organic frameworks (MOF) are considered a promising approach for photodegradation in wastewater.<sup>[3,9]</sup>

However, many investigated techniques for photocatalytic degradation of organic pollutants are activated by UV irradiation since the most efficient investigated materials are mainly based on semiconductors such as TiO<sub>2</sub>,<sup>[10]</sup> CeO<sub>2</sub>,<sup>[11]</sup> and ZnO.<sup>[12,13]</sup> To harvest irradiation in the visible light range for electrons–holes formation, the band gap ( $E_g$ ) of the photocatalyst has to be reduced. Typically, a lower  $E_g$  value is achieved by doping the semiconductor with a suitable noble metal or by forming a heterojunction by combining different photocatalysts.<sup>[14,15]</sup> The latter approach also intensifies the separation of photogenerated charge carriers leading to enhanced photocatalytic performance.<sup>[14,16–18]</sup> Nevertheless, these approaches significantly increase the process costs, thus a more economically appealing material, which is able to degrade pollutants under visible light, is needed.<sup>[9]</sup> For example, chalcogenides, which possess low band gap values by nature, are not exploited enough for the photodegradation of antibiotics. Specifically, copper sulfide is considered as a promising photocatalyst due to its economical synthesis, tunable composition, and morphology, hence has briefly revealed its potential in the degradation of antibiotics under visible light irradiation.<sup>[19,20]</sup>

It is worth noting that most of the aforementioned techniques lack sustainability because of the used harsh conditions and/or toxic fossil-based reagents.<sup>[21,22]</sup> In addition, the proposed approaches can be also very expensive on an industrial scale due to the cost of the used materials such as graphene, ozone, and MOF.<sup>[7,23]</sup> Whether adsorption membranes are applied for wastewater remediation, the antibiotics removal from the adsorbent will be mandatorily required adding a further step to the process, thus enhancing the process costs.<sup>[23]</sup> Although particle photocatalysts have achieved promising results at the lab scale, this application at the industrial level shows several drawbacks. The removal (e.g., by filtration) of the spent photocatalyst particles after wastewater treatment is a relevant issue, which further could complicate the process and cannot be ignored during the material design, especially when nano-sized particles are used as an active material for the degradation.<sup>[3]</sup>

According to the literature, few attempts have been made to make antimicrobial photodegradation more scalable. For example, to facilitate the separation of photocatalysts from wastewater, it has been previously reported the incorporation of a semiconductor in a composite material based on fossil-based matrixes (e.g., *N,N'*-dimethylacrylamide and graphitic carbon nitride).<sup>[22,20]</sup> Nevertheless, there are not enough studies reporting cost-effective organic pollutant degradation approaches, which are possible to implement on a large scale. Moreover, currently suggested technological solutions for antibiotics removal from wastewater are not suitable from the environmental point of view due to the aforementioned drawbacks. Thus, a more sustainable approach is required.

For this reason, in this work, we have combined a biopolymeric supporting material for CuS particles as a visible-light-driven photocatalyst for enhancing organic molecules degradation. Specifically, poly(3-hydroxybutyrate-co-3-hydroxyvalerate)

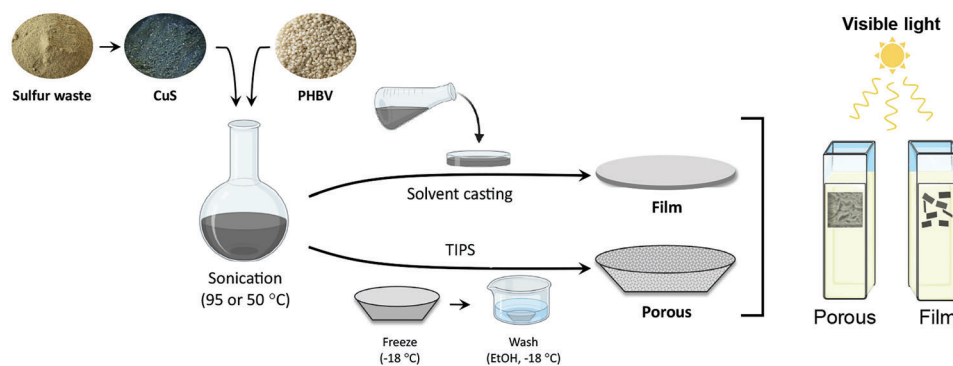
(PHBV) has been selected as supporting material, since it is one of the most promising and versatile biopolymers<sup>[24]</sup> with several potential applications<sup>[25–29]</sup> thanks to its higher ductility with respect to its homopolymers poly(3-hydroxybutyrate).<sup>[30]</sup> Moreover, PHBV is a fully bio-based and biodegradable polymer, that can be obtained by fermentation of vegetable waste.<sup>[31]</sup> In addition, this polymeric material can be easily shaped in different structures ranging from films,<sup>[32]</sup> fibers,<sup>[33]</sup> and porous architectures.<sup>[34]</sup> Due to the low band value and the possibility to be excited under visible light spectra, copper sulfide was chosen as a photocatalyst in this work. It is noteworthy that the used CuS photocatalyst is also obtained by valorizing industrial sulfur waste from sulfuric acid production, thus the final composite is a material fully obtainable from waste valorization. Since the photocatalyst particles are embedded into the polymeric matrix, the separation of the catalyst is no longer needed, thus avoiding cost-demanding procedures. The goal of this research is to produce sustainable composites with different architectures for the degradation of model pollutants such as tetracycline (TC) and methylene blue (MB). Moreover, we have also tested the recyclability of the proposed composite for a fresh stream of pollutants and its performance during the simultaneous photodegradation of a mixture of different pollutants.

## 2. Results and Discussion

Composites made of PHBV as polymeric support and CuS (15 wt% with respect to the polymer) as photocatalysts have been prepared in both films and porous structures. As summarized in **Scheme 1**, the films have been prepared by solvent casting method, whereas the porous architecture has been fabricated by the thermally induced phase separation (TIPS) method, adjusting the procedure described elsewhere to fabricate scaffolds for bone tissue regeneration.<sup>[26]</sup> In brief, first, CuS has been dispersed by dip-sonication in a PHBV solution (experimental details in Section 4). Then, the so-prepared mixture/dispersion was solidified in the freezer and afterward, the solvent was extracted from the frozen sample with ethanol by forming the porous architecture (Scheme 1).

The added CuS is synthesized by using industrial sulfur waste as a sulfuring agent, according to the method previously reported.<sup>[35]</sup> In order to validate the applicability as a waste-based photocatalyst (CuSw), we have also synthesized a reference sample of CuS by using pure sulfur, as a standard sulfurizing agent (CuSr, reference sample). The photocatalytic activity in the degradation of TC (50 mg L<sup>-1</sup>) of both photocatalysts has been tested. Furthermore, micro-fibrillated cellulose (MFC) (5 wt% with respect to the polymer) has been added to the composite formulations, to enhance the typical low hydrophilicity of PHBV, which limits the wettability of the composites by aqueous pollutants solutions (Scheme 1). The detailed composition of each prepared sample and related sample codes are presented in **Table 1**. Furthermore, representative photographs of films and porous structures are reported on the left side of **Figure 1**.

The performed XRD analysis of neat and composite samples revealed that hexagonal covellite (CuS reference pattern: PDF 04-006-9635) was the main crystalline constituent of composite samples (Figure S1, Supporting Information). This data corresponds



**Scheme 1.** Schematic representation of the sample preparation and photodegradation tests.

**Table 1.** Summary of the composition of each prepared sample.

Sample code	Sample architecture	Type of photocatalyst (sulfurizing agent)	Hydrophilicity modifier filler
CuSr/Po	Porous	Reference	–
CuSw/Po		Waste	–
CuSr/MFC/Po		Reference	MFC
CuSw/MFC/Po		Waste	MFC
PHBV/Po	Film	–	–
CuSr/Fi		Reference	–
CuSw/Fi		Waste	–
CuSr/MFC/Fi		Reference	MFC
CuSw/MFC/Fi		Waste	MFC
PHBV/Fi		–	–

perfectly with the composition of powder CuS samples reported in detail in our previous work, also proving that no new compounds were formed between polymer and photocatalyst.<sup>[35]</sup> Furthermore, all samples have been initially analyzed by field emission scanning electron microscope (FE-SEM) to investigate both the dispersion and distribution of the incorporated photocatalyst (CuS) and the formation of the desired porous structure by TIPS. Figure 1 displays the top-view FE-SEM images of film and porous composites recorded with backscattered electrons to better highlight the inorganic particles from the surrounding polymeric matrix. For both types of samples, the micrographs have revealed a homogeneous distribution and a good dispersion of CuS particles regardless of the origin of photocatalytic filler (CuSr FE-SEM images are reported in Figure S2, Supporting Information). Concerning CuSw samples, it can be noticed that the inorganic particles are less evident in CuSw/MFC/Fi compared to CuSw/Fi (Figure 1). This can be associated with the overshadowing of the CuS particles by MFC, which is composed mainly of carbon atoms, as well as the polymeric matrix. Since the surface area is much larger in porous structure than in the films, this phenomenon does not appear for porous samples. Most importantly, it is evident that the high interconnected porosity of porous composites with homogeneously distributed CuS has been achieved (Figure 1). Moreover, the FE-SEM images of film cross-sections have shown that CuS particles have only partially aggregated throughout the film's thickness (Figure S3, Supporting Information).

The photocatalytic activity of the prepared composite material has been evaluated by investigating the degradation efficiency of tetracycline as a model antibiotic pollutant, under visible light irradiation that activates the photocatalytic activity of CuS. In particular, the degradation efficiency was determined by measuring the absorbance peak centered at 351 nm of TC solution (50 mg L<sup>-1</sup>) containing the composite sample immersed in the cuvette (representative spectra at different timepoints reported in Figure S4, Supporting Information) by UV-vis spectroscopy (more experimental details in Section 4, and the experimental setup is shown in Figure S5, Supporting Information).

The obtained kinetic curves of TC degradation under visible light with porous or film composites as photocatalysts are reported in Figure 2 (standard deviations for each experimental point of Figure 2 are reported in Table S1, Supporting Information, in order to have more readable plots). According to the degradation efficiency data, it is observed that the majority of tested samples have reached the 100% of degradation efficiency within 180 min of photooxidation regardless of the sample architecture (Figure 2A,B). Furthermore, no significant differences in degradation efficiency have been noticed whether using CuS synthesized from waste or a reference sulfurizing agent. As a representative, CuSr/Po and CuSw/Po samples are able to degrade 56% and 60% of pollutants, respectively, after 120 min (Figure 2A). Photodegradation has a similar initial reaction rate by both waste and reference samples with porous architecture. On the other hand, when reference and waste photocatalysts are

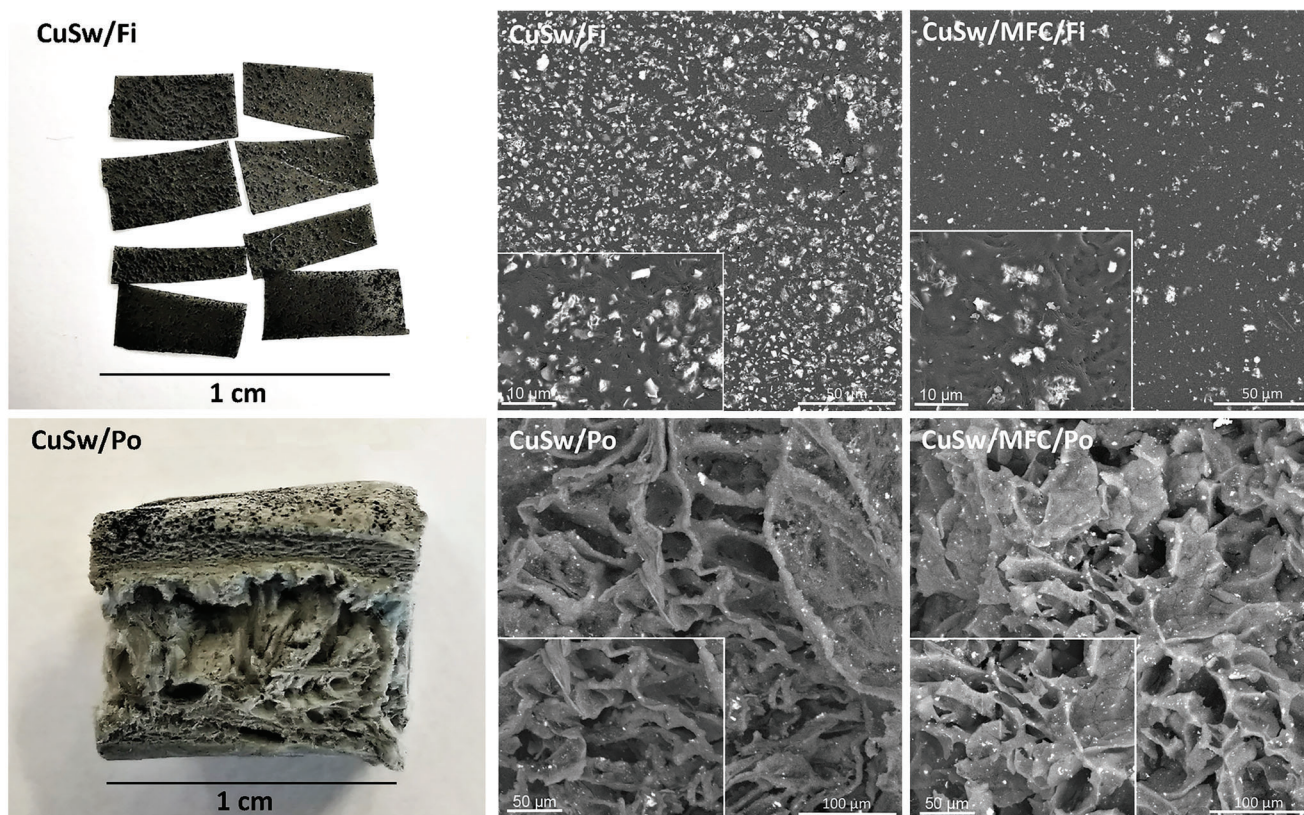


**Figure 1.** On the left: representative photographs of porous and film PHBV/CuS composites. On the right: FE-SEM top-view images (back-scattered electrons) of film and porous composites with CuSw and MFC as fillers.

embedded in films, the degradation rate reaches a value 1.4 times higher with CuS particles obtained from waste (CuSw/Fi sample –  $0.5203 \text{ min}^{-1}$ ; CuSr/Fi –  $0.3834 \text{ min}^{-1}$ ) (Figure 2C,D). It is known from previous work<sup>[35]</sup> that CuSw has a larger crystallite average size than CuSr (39 and 35 nm, respectively), which can result in a higher degradation rate as reported by Goktas et al.<sup>[36]</sup> in their work on ZnO.

The well-known high hydrophobicity of PHBV can slow down the kinetic degradation, limiting the contact between the aqueous pollutant solution and photocatalyst. As a possible solution, we tried to reduce the water contact angle (WCA) of PHBV by adding MFC, which can decrease the typical high hydrophobicity of PHBV thanks to the hydroxyl groups in its structure as also observed for other polymers.<sup>[37]</sup> In addition, a positive influence on TC degradation can be observed when MFC is incorporated into the porous composites, leading to a degradation efficiency that is enhanced by up to 13% throughout the whole irradiation time (Figure 2A). It is also important to underline that the initial reaction rate constant is 3.3 and 4.2 times higher for CuSr/MFC/Po and CuSw/MFC/Po samples, respectively, compared to the samples without MFC (Figure 2C). This confirms that photocatalytic reaction is more rapid in the presence of MFC-modified porous samples (Figure 2C). In particular, the MFC significantly increases the wettability of porous composites by  $11^\circ$  (WCA data in Figure 3 and Table S2, Supporting Information) and consequently leads to an increase of the permeability of the

porous structure by the TC aqueous solution and thus increases the active surface of the sample exposed to the solution.

On the contrary, MFC has a negative influence on degradation efficiency by film composites when both types of photocatalysts are used (Figure 2B). More in detail, it is observed that 100% degradation efficiency is achieved after 150 min of irradiation by the sample without MFC (CuSw/Fi and CuSr/Fi). While, by using the MFC-modified film composites, TC complete degradation is achieved 30 min later (Figure 2B).

The reaction rate constants are also slightly lower by 12% and 24% for CuSr/MFC/Fi and CuSw/MFC/Fi, respectively (Figure 2D). In the film samples, both types of fillers are distributed throughout a flat substrate, which has less free surface area compared to the composite with a porous structure. In the film samples, the photocatalyst particles are more likely partially shielded by MFC than in porous structure, resulting in less concentrated exposed particles on the surface as shown by FE-SEM investigations (Figure 1). This result in lowering the number of electrons/holes, which are involved in photodegradation, thus leading to an overall lowering of the degradation efficiency. Besides, it has been observed that the MFC only slightly affects the hydrophobicity of the film samples with a reduction of WCA of only  $4^\circ$  (Figure 3 and Table S2, Supporting Information). The very low standard deviations of the WCA measurements (Figure 3) also provide indirect information about the MFC homogeneous distribution and the effectiveness of the MFC dispersion method,

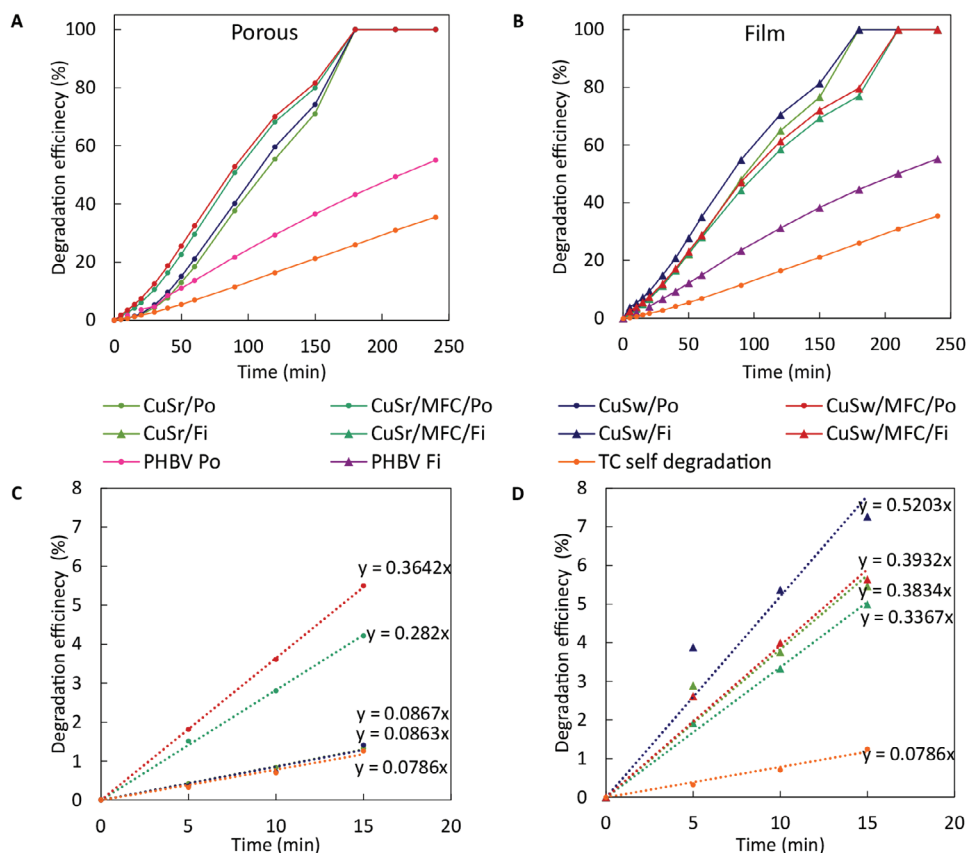


**Figure 2.** Degradation efficiency as a function of the time evaluated by degrading TC under visible light with A) porous and B) film composites immersed in the solution. Pseudo-first order kinetic curves of TC photocatalytic degradation by C) porous and D) film composites.

considering that each WCA measurement is the average of five repetitions in different parts of the sample surface.

The architecture of the composite also affects the photodegradation rate. It was observed that photodegradation is significantly faster in the film than in porous samples, with the initial reaction rate constant of  $0.083 \text{ min}^{-1}$  for CuSw/Po and  $0.5203 \text{ min}^{-1}$  for CuSw/Fi, which is about six times higher (Figure 2C,D). The addition of MFC increases the degradation rate of porous composites up to a rate comparable with film samples of equal composition. Specifically, the initial reaction rate achieved with CuSw/MFC/Fi and CuSw/MFC/Po is  $0.3932$  and  $0.3642 \text{ min}^{-1}$ , respectively (Figure 2C,D).

Since the tests of TC photocatalytic degradation by composites with waste-based CuS have shown results very similar to the CuS prepared from reference sulfurizing agent (Figure 2), and taking into account the sustainability point of view, only composites with CuS from sulfur waste valorization have been selected for further investigations. Furthermore, due to the highest initial reaction rate and degradation efficiencies throughout the whole irradiation time, only CuSw/MFC/Po and CuSw/Fi samples have been further analyzed.

The reusability of composites for the photodegradation of fresh batches of pollutants is another key parameter to evaluate. The research findings have shown that both CuSw/MFC/Po and CuSw/Fi samples can be reused at least five times, reaching 100% of TC degradation after each cycle (Figure 4A,B). Specifi-

cally, after 60 min of irradiation during the first cycle, the degradation efficiency is 33% and 37% for CuSw/MFC/Po and CuSw/Fi, respectively (Figure 4C,D). It is worth noting that both samples double their degradation efficiency during the second photodegradation cycle achieving, after 60 min of irradiation, values of 61% and 75% for CuSw/MFC/Po and CuSw/Fi, respectively (Figure 4C,D). Furthermore, during the second cycle, 100% of TC degradation is achieved 30 min quicker than during the first cycle by both samples (Figure 4C,D).

Most importantly, the evident performance enhancement of pollutant photodegradation by both sample types is achieved. It has been seen that, in the second cycle, the initial reaction rate constant obtained using CuSw/MFC/Po has increased 2.5 times from  $0.3642 \text{ min}^{-1}$  to a value of  $0.9036 \text{ min}^{-1}$  (Figure 4E). A comparable increase is also observed for CuSw/Fi sample with the reaction rate constant that increases by 2.3 times reaching a value of  $1.2051 \text{ min}^{-1}$  compared to the value that has been recorded during the first cycle of photodegradation ( $0.5203 \text{ min}^{-1}$ ) (Figure 4E). Accordingly, both tested samples also show performance enhancement in the values of degradation efficiency.

This unexpected behavior suggests that during the second cycle, the photodegradation already starts by harvesting the charge carriers, which were generated during the first cycle and then were trapped in the subsurface of the semiconductor.<sup>[38]</sup> Regardless of the used composite, after the second cycle, the reaction rate constant starts gradually decreasing. This is even more

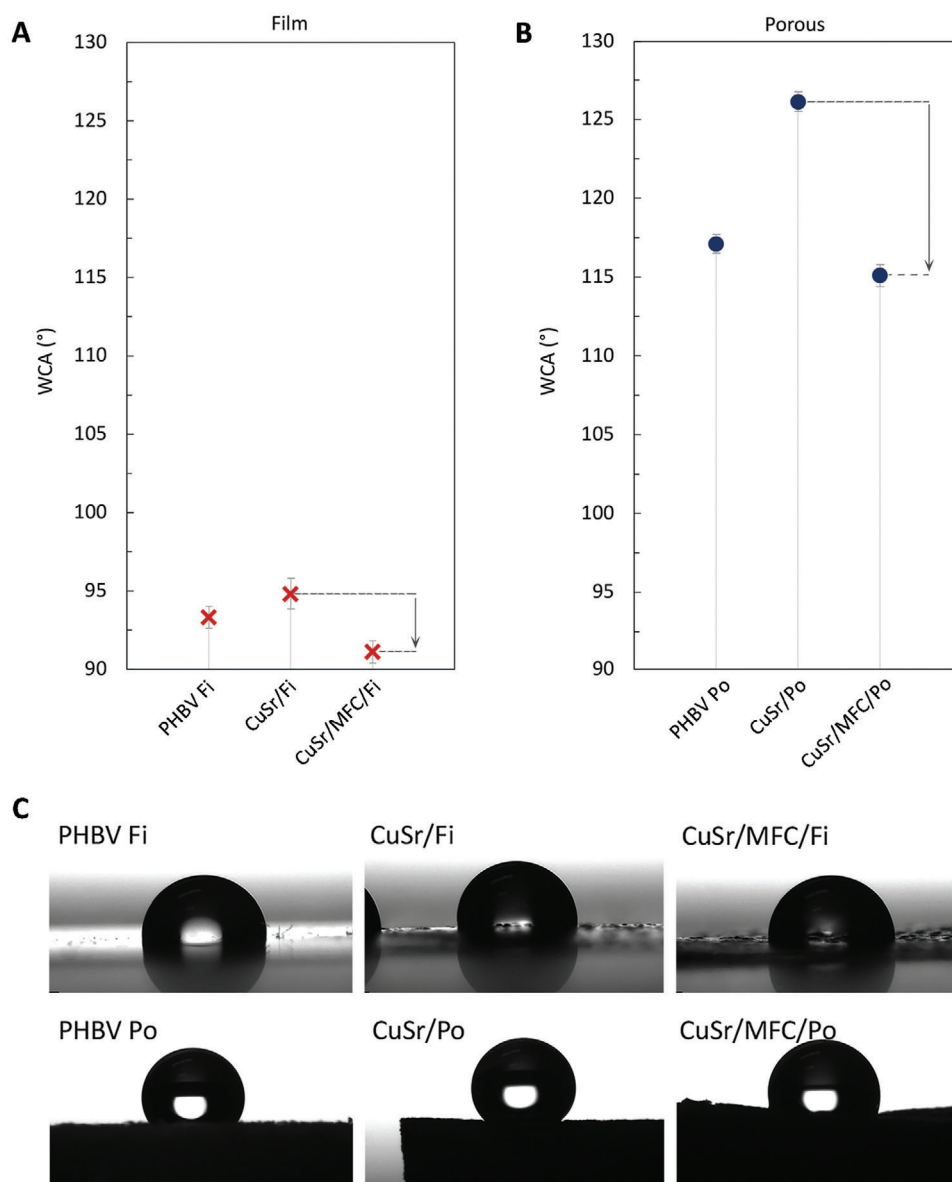


**Figure 3.** Water contact angle (WCA) of A) films and B) porous structures of neat PHBV and composites with and without MFC. C) Representative images of water drop used for the shape analysis under static conditions to determine the contact angle on the different tested samples.

visible from the third cycle when the photocatalyst begins losing efficiency according to the previously reported phenomenon called mild photocorrosion of CuS.<sup>[9,39,22]</sup> Specifically, during this process, the generated charge carriers oxidize the sulfur ions of CuS, thereby resulting in the loss of photocatalyst active sites, as observed elsewhere.<sup>[40]</sup>

However, the photodegradation occurs with a slightly higher reaction rate during the last four cycles in comparison with the first one (as shown in Figure 4E). Also, the degradation efficiency, by both composites at 60 min of irradiation, decreases by 20% within reusability experiments (Figure 4C,D). Nevertheless, the value is still higher compared to the first cycle by 18% and 5% for CuSw/Fi and CuSw/MFC/Po, respectively (Figure 4C,D). This data also suggests that the holes and electrons are trapped on

the surface of the photocatalyst. Specifically, since the lifetime of trapped charge carriers on the surface can be even up to months, the immediate generation of radicals proceeds during the repetitive cycle of photodegradation.<sup>[38]</sup> Thus, this phenomenon leads to a higher degradation efficiency and faster degradation rate obtained while reusing the composites compared to the first application of the sample. Most importantly, 100% of TC degradation is achieved after 150 min of visible light irradiation by CuSw/Fi composite and the same result is maintained even after the fifth cycle of composite usage (Figure 4D). Most of the studies that use free particles show indeed a very fast degradation rate, but also a loss of efficiency already after the first cycle.<sup>[41–44]</sup> The chemical stability of the herein-used photocatalyst was also confirmed by XRD analysis on the composite before and after five cycles.

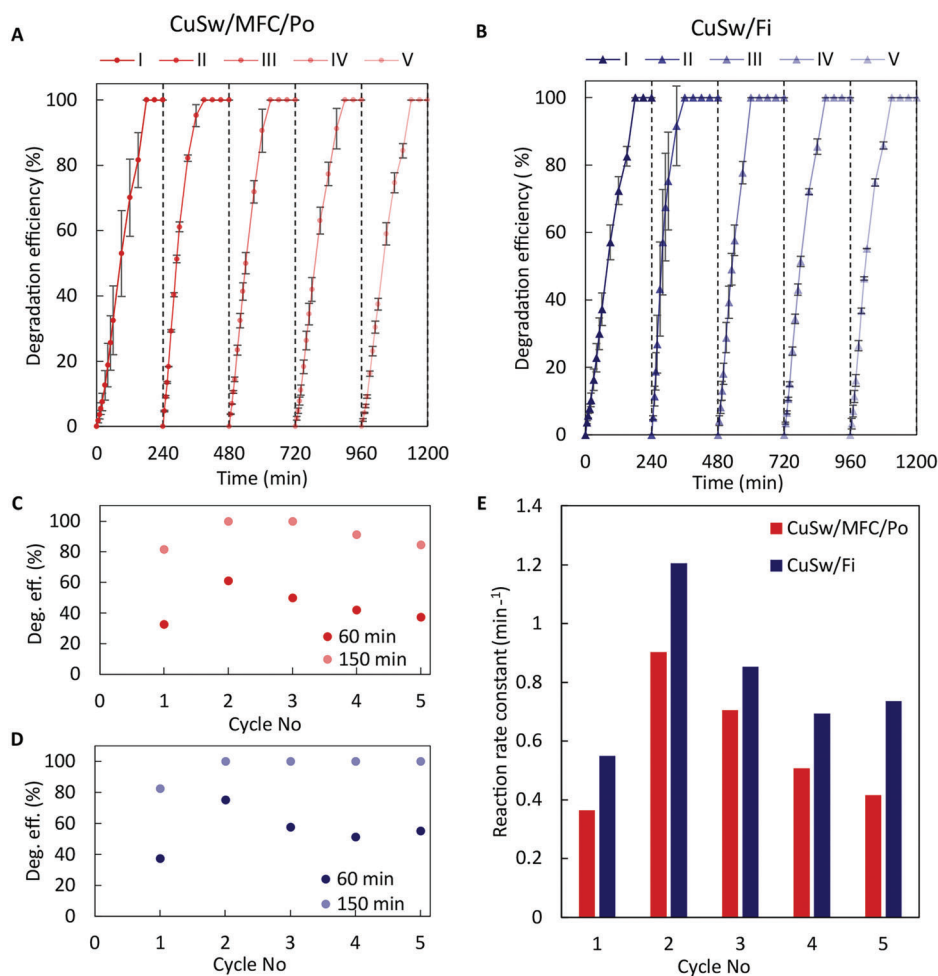


**Figure 4.** Degradation efficiency obtained by degrading TC with A) CuSw/MFC/Po and B) CuSw/Fi composites by reusing each sample for five cycles. Degradation efficiency as a function of the number of cycles for C) CuSw/MFC/Po and D) CuSw/Fi samples after 60 and 150 min of irradiation. E) Reaction rate constant as a function of the number of cycles for CuSw/MFC/Po and CuSw/Fi.

The XRD results (Figure S1, Supporting Information) revealed the same chemical compound composition in the CuSw/Fi sample (as representative) even after five cycles of TC photodegradation, suggesting that the polymer has a protective effect on the CuS particles.

The potentiality of the prepared composites to simultaneously degrade different pollutants in the same solution has been further investigated. For this reason, CuS/MFC/Po and CuSw/Fi samples have been tested to photodegrade MB (10 mg L<sup>-1</sup>) and TC (100 mg L<sup>-1</sup>) model pollutants in a mixture under visible light.

The results revealed that both pollutants are simultaneously degraded by both CuSw/MFC/Po and CuSw/Fi composites. During the whole irradiation, the degradation efficiency for TC and MB is higher for porous samples compared to films (Figure 5A,B). In particular, after 150 min of irradiation, CuSw/Fi composite has degraded 78.5% of TC and 89.9% of MB, whereas the degradation efficiency obtained by CuSw/MFC/Po is 5.7% and 6.3% higher, respectively (Figure 5A,B). Furthermore, the reaction rate constant achieved by CuSw/Fi sample was 0.6979 and 0.5635 min<sup>-1</sup> for TC and MB, respectively (Figure 5C,D). Interestingly, we have noticed that photodegradation started faster in

the porous composite than in the film sample with a reaction rate constant that achieved, for CuSw/MFC/Po sample, 0.8044 and 0.6744 min<sup>-1</sup> for TC and MB, respectively (Figure 5C,D). Nevertheless, both types of samples achieve 100% of photodegradation for both model pollutants within 210 min (Figure 5A,B), showing no significant differences for this experiment.

It is also worth noting that for this experiment, we have doubled the TC concentration (from 50 to 100 mg L<sup>-1</sup>). Despite that, both samples lead to a complete pollutant degradation within 210 min. By increasing TC concentration, the reaction rate constant achieved by CuSw/Fi has increased 1.4 times, and the value obtained by CuSw/MFC/Po composite has doubled (Figure S6, Supporting Information), confirming that the composites are suitable to degrade even higher concentrations of TC.

### 3. Conclusions

In this work, sustainable PHBV/CuS composites have been developed for the purification of organic pollutants from wastewater by photodegradation. The proposed materials can be fully

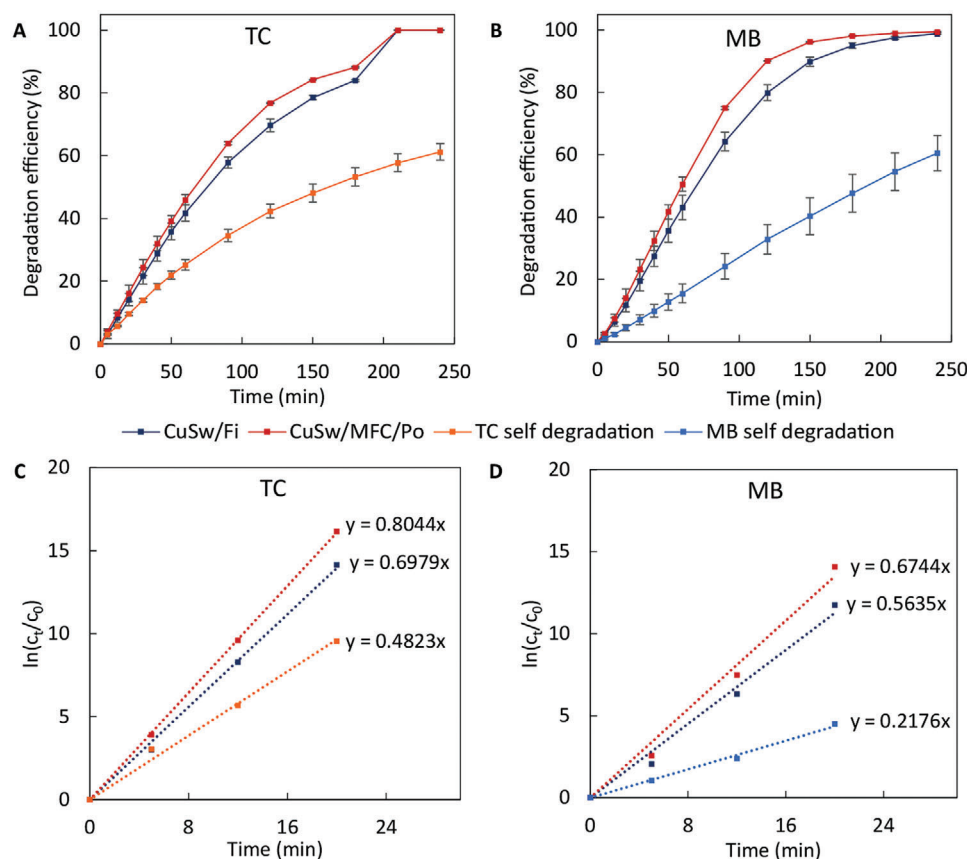


**Figure 5.** Degradation efficiency obtained with CuSw/MFC/Po and CuSw/Fi composites by simultaneous degradation of A) tetracycline (TC) and B) methylene blue (MB). Pseudo-first order kinetic curves of photocatalytic simultaneous degradation of C) tetracycline (TC) and D) methylene blue (MB) by CuSw/MFC/Po and CuSw/Fi.

obtained from the valorization of by-products or wastes of other production. In particular, the investigation is focused on tetracycline photodegradation activated by visible light irradiation and catalyzed by the produced composites both in film and porous structure. The research findings have shown that the composites, prepared from the valorization of sulfur waste, are not only eligible to degrade organic pollutants but also have shown a higher degradation efficiency and faster kinetics than the composite with CuS obtained from conventional sulfur sources. It was also determined that the hydrophilicity modifier (microfibrillated cellulose, MFC) had a positive influence only on porous composites significantly decreasing the typical high WCA of the PHBV polymeric support. In addition, the highest degradation efficiency and the fastest initial photodegradation kinetics are achieved by samples with CuS obtained from industrial waste in film and with porous architecture modified with microfibrillated cellulose. It is noteworthy that the latter samples have degraded 100% of tetracycline within 180 min of visible light irradiation.

Furthermore, it was observed that the produced composites can be reused for at least five cycles and continue to reach 100% of degradation efficiency. Besides, the investigation of composite reusability has also revealed the enhancement of photodegradation performance within the second cycle, since 100% of pollutant degradation was achieved 30/60 min earlier compared to the data obtained during the first cycle.

Simultaneous photodegradation experiments of two different types of model pollutants have been also carried out. It has been observed that produced composites can efficiently and simultaneously photodegrade both methylene blue and tetracycline achieving 100% degradation for both pollutants in 240 min of irradiation. Since the concentration of tetracycline in this experiment is double that in the initial experiments ( $100 \text{ mg L}^{-1}$  instead of  $50 \text{ mg L}^{-1}$ ), it can be concluded that the PHBV/CuS composites can efficiently degrade tetracycline even in higher concentrations.

The presented approach for organic molecules photodegradation under visible light catalyzed by composites produced from waste materials represents a very efficient method not only to valorize waste but also to face current issues concerning wastewater treatment. The simplicity of the proposed systems and the only need for visible light to be activated are important factors that make affordable their scale up. Furthermore, model pollutants that are used in this study as proof of concept demonstrated that different types of organic molecules can be efficiently degraded also when they are in a mixture. However, several other types of organic pollutants can be treated using the PHBV/CuS composites, thus opening up a novel route to exploit biopolymer-supported semiconductor particles for water remediation, thus avoiding further steps as filtration, at the end of the process.



## 4. Experimental Section

**Materials:** PHBV, (custom grade, Mn 209300, Mw 586000, 20 mol% 3HV unit) was purchased from Merck and purified before further treatment as described in previous work.<sup>[26]</sup> Copper sulfide (CuS) was synthesized hydrothermally in an aqueous solution regardless of the used sulfuring agent (sulfur waste/reference). The dominant diameter of both waste and reference copper sulfide particles was 22–50 μm (particle size distribution in Figure S7, Supporting Information). A detailed description of CuS synthesis is previously reported elsewhere.<sup>[35]</sup> Dry MFC was used as a hydrophilicity enhancer, which was produced by a previously established method reported elsewhere.<sup>[45]</sup>

Chloroform (CHCl<sub>3</sub>, HPLC grade), 1,4-dioxane (DIOX, ≥99%), ethyl alcohol (EtOH, ≥99.8%), hydrogen peroxide (H<sub>2</sub>O<sub>2</sub>, 30%), MB (C<sub>16</sub>H<sub>18</sub>ClN<sub>3</sub>S·3H<sub>2</sub>O), and TC (C<sub>22</sub>H<sub>24</sub>N<sub>2</sub>O<sub>8</sub>·HCl, analytical standard) were purchased from Merck Group, Italy.

**Samples Preparation:** The porous composites were prepared by dispersing CuS particles (15 wt% with respect to the polymer) in a purified PHBV/DIOX solution (1.08 g of PHBV in 30 mL of solvent). In particular, the mixing was performed by coupling magnetic stirring with dip-sonication (ultrasonic processor UP50H, Hielscher, sonotrode MS2 operating at 50 W and 30 kHz) for 3 h. The procedure was performed at 104 °C, under reflux. After the dispersion step, the porous structure of the composite was obtained by the TIPS technique.<sup>[26]</sup> First, the dispersed suspension was poured into a circular aluminum mold (diameter 55 mm, height 10 mm) and maintained at –18 °C temperature for 18 h. Then, the frozen sample was extracted from the mold and immersed in an ethanol bath at –18 °C to extract DIOX from the composite structure. Cold ethanol was refreshed every 24 h for two times. Afterward, the formed porous structure was rinsed with distilled water in an ultrasound bath and dried in an oven at 50 °C for 24 h (representative photographs of the samples are reported in Figure 1, left side).

In order to increase the hydrophilicity of samples, 5 wt% of MFC (with respect to the polymer) was added to the dispersion before sonication to enhance the wettability of the composite.

The composite film was prepared by solvent casting using chloroform as a solvent with the same formulation prepared for the porous materials. In detail, CuS and MFC were first dispersed for 3 h by dip-sonication combined with magnetic stirring at 50 °C and consequently cast in a Petri dish of 11 cm diameter and finally left drying at room temperature overnight.

Moreover, neat PHVB samples in both film and porous structures were prepared for comparison reasons. Representative photographs of the two types of samples are reported in Figure S8, Supporting Information.

**Photodegradation Experiments:** The photodegradation experiments were performed in a 4 mL quartz cuvette in stirred solutions under irradiation of visible light (irradiation centered at λ > 420 nm, Philips PL-S, 900 lm). 3 mL of TC solution (50 mg L<sup>-1</sup>) was mixed with 60 μL of H<sub>2</sub>O<sub>2</sub>. The porous composite sample was prepared in a 1 × 1 × 1 cm<sup>3</sup> size cube and immersed into the pollutant solution. The average mass of each sample was ≈0.04 g. The film composite sample was prepared in a 1 cm<sup>2</sup> area, then cut into eight equal pieces, and immersed into the experimental solution. The average mass of the sample was 0.01 g. Before starting the irradiation, the samples were left in the dark for 10 min to reach the adsorption/desorption equilibrium. The negligible decrease of UV–vis absorbance peak was achieved during the experiment in the dark (Figure S9, Supporting Information). The solution was then exposed to visible light irradiation by the light source which was placed 4 cm above the surface of the experimental solution. After each specified irradiation interval, the concentration of pollutant was determined by measuring the UV–vis absorption peak at 351 nm characteristic of TC (Figure S4, Supporting Information). UV–vis absorption spectra of pollutant solutions were measured with a UV–vis spectrophotometer (JASCO, V-650). The DE was calculated by using the following formula

$$DE = (1 - A_t/A_0) \times 100 \quad (1)$$

where  $A_t$  represents the absorbance at a generic timepoint and  $A_0$  is the initial absorbance value before starting the light irradiation.

The reaction rate constant was calculated from the initial linear part of the kinetic curves using the points collected in the first 15 min. The values were obtained by fitting the linear part of the pseudo-first-order kinetic model with a high correlation coefficient ( $R^2$ ) (all values are reported in Tables S3–S5, Supporting Information).

$$\ln(C_t/C_0) = -kt \quad (2)$$

where  $t$  is the time interval and  $k$  is the reaction rate constant.

For investigation of composites reusability, CuSw/MFC/Po and CuSw/Fi samples were completely dried at room temperature after the first photodegradation experiment and then further reused for four batches of fresh pollutant solution.

Furthermore, photodegradation activity was also determined in a mixture of different pollutants. In detail, the mixture of pollutants was prepared with 100 mg L<sup>-1</sup> of TC and 10 mg L<sup>-1</sup> of MB. Photodegradation experiments were carried out using the same procedure and conditions described above. To determine the concentration of MB, the characteristic absorption peak, centered at 664 nm, was used. Moreover, for comparison reasons, the photodegradation of TC and TC/MB solutions was performed without any photocatalyst by running blank tests and also with neat polymer samples.

Each photodegradation experiment was repeated three times. The average values are presented in the figures, whereas the standard deviations are presented in Tables S1, S6, and S7, Supporting Information, to avoid overcrowding the images.

**Characterizations:** Field emission scanning electron microscopy (FE-SEM, Mira3, Tescan) was used to investigate the formation of the porous structure and the filler distribution in the polymer matrix. Cross sections of the film composites were prepared by cryo-fracturing the samples in liquid nitrogen. All samples were then attached on an aluminum stub by a conductive carbon tab and coated by the electro-deposition method with ≈10 nm of gold. The cross-section and top-view images of films were examined by applying an accelerating voltage of 20 kV with a backscattered electron detector. The porous composites were analyzed by low vacuum mode by applying an accelerating voltage of 10 kV.

The static WCA measurements were carried out by a KRUSS, DSA30 contact angle goniometer equipped with a digital camera. 4 μL of Milli-Q water droplets were deposited on the surface of the composite samples. The presented average values and standard deviations were calculated out of five measurements.

## Supporting Information

Supporting Information is available from the Wiley Online Library or from the author.

## Acknowledgements

This research was funded by the Doctoral Fund of the Kaunas University of Technology, No-410, approved on 26 June 2019. G.S. acknowledges the ERASMUS+traineeship program (Grant No 2020-1-LT01-KA103-0775220), through Lithuania, which supported student's visits to the University of Bologna. The authors are also thankful to Mr. Giovanni Ridolfi for technical support in the XRD investigations reported in Supporting Information.

## Conflict of Interest

The authors declare no conflict of interest.

## Author Contributions

G.S.: Investigation, writing – original draft preparation, data curation, visualization, writing – review & editing; K.B.: Resources; M.D.E.:

Investigation, writing – original draft preparation, supervision; D.M.: Conceptualization, supervision, writing – original draft preparation, data curation, visualization, writing – review & editing; P.F.: Resources.

## Data Availability Statement

The data that support the findings of this study are available from the corresponding author upon reasonable request.

## Keywords

antibiotics, copper sulfide, photooxidation, polyhydroxyalkanoates, polymer composites, waste valorization, wastewater remediation

Received: March 17, 2023

Revised: May 26, 2023

Published online:

- [1] World Health Organization, Technical brief on water sanitation, hygiene, and wastewater management to prevent infections and reduce the spread of antimicrobial resistance, Geneva, **2020**.
- [2] United Nations, The Sustainable Development Goals Report, **2022**.
- [3] C. Bhagat, M. Kumar, V. K. Tyagi, P. K. Mohapatra, *npj Clean Water* **2020**, *3*, 42.
- [4] E. Tacconelli, F. Sifakis, S. Harbarth, R. Schrijver, M. van Mourik, A. Voss, M. Sharland, N. B. Rajendran, J. Rodríguez-Baño, J. Bielicki, M. de Kraker, S. Gandra, P. Gastmeier, K. Gilchrist, A. Gikas, B. P. Gladstone, H. Goossens, H. Jafri, G. Kahlmeter, F. Leus, C. Luxemburger, S. Malhotra-Kumar, G. Marasca, M. McCarthy, M. D. Navarro, M. Nuñez-Nuñez, A. Oualim, J. Price, J. Robert, H. Sommer, et al., *Lancet Infect. Dis.* **2018**, *18*, e99.
- [5] World Health Organization, Antibiotics resistance, **2020**.
- [6] J. Yu, Y. Kang, W. Yin, J. Fan, Z. Guo, A. C. S. Omega, **2020**, *5*, 19187.
- [7] J. Yang, S. Shojaei, S. Shojaei, *npj Clean Water* **2022**, *5*, 5.
- [8] M. S. de Ilurdoz, J. J. Sadhwani, J. V. Reboso, *J. Water Process Eng.* **2022**, *45*, 102474.
- [9] V. I. Parvulescu, F. Epron, H. Garcia, P. Granger, *Chem. Rev.* **2022**, *122*, 2981.
- [10] D. Morselli, M. Messori, F. Bondioli, *J. Mater. Sci.* **2011**, *46*, 6609.
- [11] D. Morselli, L. Campagnolo, M. Prato, E. L. Papadopoulou, A. Scarpellini, A. Athanassiou, D. Fragouli, *ACS Appl. Nano Mater.* **2018**, *1*, 5601.
- [12] M. Ahmed, M. O. Mavukkandy, A. Giwa, M. Elektorowicz, E. Katsou, O. Khelifi, V. Naddeo, S. W. Hasan, *npj Clean Water* **2022**, *5*, 12.
- [13] W. Liu, T. He, Y. Wang, G. Ning, Z. Xu, X. Chen, X. Hu, Y. Wu, Y. Zhao, *Sci. Rep.* **2020**, *10*, 11903.
- [14] K. Balu, E. Chicardi, R. Sepúlveda, M. Durai, F. Ishaque, D. Chauhan, Y.-H. Ahn, *Sep. Purif. Technol.* **2023**, *309*, 122998.
- [15] C. Wang, R. Yan, M. Cai, Y. Liu, S. Li, *Appl. Surf. Sci.* **2023**, *610*, 155346.
- [16] M. Cai, Y. Liu, C. Wang, W. Lin, S. Li, *Sep. Purif. Technol.* **2023**, *304*, 122401.
- [17] S. Li, M. Cai, C. Wang, Y. Liu, *Adv. Fiber Mater.* **2023**, *5*, 994.
- [18] M. Cai, C. Wang, Y. Liu, R. Yan, S. Li, *Sep. Purif. Technol.* **2022**, *300*, 121892.
- [19] S. Sun, P. Li, S. Liang, Z. Yang, *Nanoscale* **2017**, *9*, 11357.
- [20] M. J. F. Calvete, G. Piccirillo, C. S. Vinagreiro, M. M. Pereira, *Coord. Chem. Rev.* **2019**, *395*, 63.
- [21] M. Kamranifar, A. Allahresani, A. Naghizadeh, *J. Hazard. Mater.* **2019**, *366*, 545.
- [22] X. Guo, F. Yang, X. Sun, C. Han, Y. Bai, G. Liu, W. Liu, R. Wang, *J. Mater. Chem. A* **2022**, *10*, 3146.
- [23] M. Gheytnzadeh, A. Baghban, S. Habibzadeh, K. Jabbour, A. Esmaeili, A. Mohaddespour, O. Abida, *Sci. Rep.* **2022**, *12*, 6615.
- [24] Z. Li, J. Yang, X. J. Loh, *NPG Asia Mater.* **2016**, *8*, e265.
- [25] K. Papchenko, M. Degli Esposti, M. Minelli, P. Fabbri, D. Morselli, M. G. de Angelis, *J. Memb. Sci.* **2022**, *660*, 120847.
- [26] M. Degli Esposti, M. Changizi, R. Salvatori, L. Chiari, V. Cannillo, D. Morselli, P. Fabbri, *ACS Appl. Polym. Mater.* **2022**, *4*, 4306.
- [27] C. de Maria, I. Chiesa, D. Morselli, M. R. Ceccarini, S. Bittolo Bon, M. Degli Esposti, P. Fabbri, A. Morabito, T. Beccari, L. Valentini, *Adv. Funct. Mater.* **2021**, *31*, 2105665.
- [28] S. B. Bon, I. Chiesa, M. Degli Esposti, D. Morselli, P. Fabbri, C. de Maria, A. Morabito, R. Coletta, M. Calamai, F. S. Pavone, R. Tonin, A. Morrone, G. Giorgi, L. Valentini, *ACS Appl. Mater. Interfaces* **2021**, *13*, 21007.
- [29] P. Cataldi, P. Steiner, T. Raine, K. Lin, C. Kocbas, R. J. Young, M. Bissett, I. A. Kinloch, D. G. Papageorgiou, *ACS Appl. Polym. Mater.* **2020**, *2*, 3525.
- [30] I. Chodak, in *Monomers, Polymers, and Composites from Renewable Resources* (Eds.: M. N. Belgacem, A. Gandini), Elsevier, Amsterdam **2008**, pp. 451–477.
- [31] M. Koller, R. Bona, G. Braunegg, C. Hermann, P. Horvat, M. Kroutil, J. Martinz, J. Neto, L. Pereira, P. Varila, *Biomacromolecules* **2005**, *6*, 561.
- [32] S. B. Bon, L. Valentini, M. D. Esposti, D. Morselli, P. Fabbri, V. Palazzi, P. Mezzanotte, L. Roselli, *J. Appl. Polym. Sci.* **2021**, *138*, 49726.
- [33] L. Brunetti, M. Degli Esposti, D. Morselli, A. R. Boccaccini, P. Fabbri, L. Liverani, *Mater. Lett.* **2020**, *278*, 128389.
- [34] M. D. Esposti, F. Chiellini, F. Bondioli, D. Morselli, P. Fabbri, *Mater. Sci. Eng., C* **2019**, *100*, 286.
- [35] G. Sarapajevaite, D. Morselli, K. Baltakys, *Materials* **2022**, *15*, 5253.
- [36] A. Goktas, S. Modanlı, A. Tumbul, A. Kilic, *J. Alloys Compd.* **2022**, *893*, 162334.
- [37] X. Sun, C. Mei, A. D. French, S. Lee, Y. Wang, Q. Wu, *Cellulose* **2018**, *25*, 5071.
- [38] L. Zhang, H. H. Mohamed, R. Dillert, D. Bahnemann, *J. Photochem. Photobiol., C* **2012**, *13*, 263.
- [39] M. Maleki, M. Haghighi, *J. Mol. Catal. A: Chem.* **2016**, *424*, 283.
- [40] S. Chen, D. Huang, P. Xu, W. Xue, L. Lei, M. Cheng, R. Wang, X. Liu, R. Deng, *J. Mater. Chem. A* **2020**, *8*, 2286.
- [41] E. V. Siddhardhan, S. Surender, T. Arumanayagam, *Inorg. Chem. Commun.* **2023**, *147*, 110244.
- [42] C. Lai, F. Xu, M. Zhang, B. Li, S. Liu, H. Yi, L. Li, L. Qin, X. Liu, Y. Fu, N. An, H. Yang, X. Huo, X. Yang, H. Yan, *J. Colloid Interface Sci.* **2021**, *588*, 283.
- [43] Y. Wang, Q. Liu, N. H. Wong, J. Sunarso, J. Huang, G. Dai, X. Hou, X. Li, *Ceram. Int.* **2022**, *48*, 2459.
- [44] P. Nandi, D. Das, *J. Phys. Chem. Solids* **2022**, *160*, 110344.
- [45] T. Saito, Y. Nishiyama, J.-L. Putaux, M. Vignon, A. Isogai, *Biomacromolecules* **2006**, *7*, 1687.